AAS 19-567

OBJECTIVE FUNCTION WEIGHT SELECTION FOR SEQUENTIAL LOW-THRUST ORBIT-RAISING OPTIMIZATION PROBLEM

Atri Dutta* **and Lakshay Arora†**

In this paper, we consider the low-thrust orbit-raising problem formulated as a sequence of optimal control sub-problems. This formulation is helpful in rapid and robust generation of geocentric electric orbit-raising trajectories, however this advantage comes at the cost of sub-optimality of the computed solutions. The objective function that is minimized in each optimal control sub-problem is a convex combination of components and reflects the deviation of the maneuvering spacecraft from the geosynchronous equatorial orbit. This paper explores the impact of weights the objective function components on the optimality gap of computed orbit-raising trajectories, and numerical examples based on a variety of orbit-raising scenarios are used to illustrate this effect.

INTRODUCTION

The use of of electric propulsion (EP) for the purpose of orbit-raising of telecommunication satellites to the geosynchronous equatorial orbit (GEO) allows for the design of smaller and lighter satellites, by taking advantage of the superior propellant management of EP over traditional chemical propulsion systems. Naturally, there has been a tremendous surge in interest among satellite operators across the globe in incorporating EP system in their satellites for the purpose of transferring to the GEO. In 2015, the first-ever all-electric satellites (operated by SatMex and ABS) incorporating Boeing 702-SP all-electric architecture were successfully deployed in GEO. In 2017, the same feat was accomplished by Eutelsat 172B satellite that incorporates the fully electric architecture built by Airbus. In Asia, China also have started incorporating EP in their indigenous satellites, as demonstrated by the SJ-13 mission in 2017. While initial developments have been aimed primarily at small- and medium-platform satellites, it is likely, that the space industry will see the incorporation of all-electric propulsion architecture within high power telecommunication satellites in the future. Owing to the low thrust producing capacity of EP thrusters, the design of the mission of an all-electric spacecraft has its challenges, mostly stemming from the large transfer times associated with long transfers spanning several months. The long transit time through the surrounding Van Allen radiation belts results in significant damage to the solar arrays of the satellite. The multiple eclipses encountered en route by the satellite only complicates an already long transfer time. A mission designer therefore needs to investigate a variety of mission scenarios in order to decide on a number of key factors affecting the electric orbit-raising mission (see Fig. 1): starting orbit for the EP-based transfer, launch vehicle selection (affecting the starting mass), solar array shielding requirements (affects power loss and thereby thrusting capability

*Assistant Professor, Aerospace Engineering, Wichita State University, 1845 Fairmount St Box 42, Wichita KS 67260.
†M.S. Student, Aerospace Engineering, Wichita State University, 1845 Fairmount St Box 42, Wichita KS 67260.

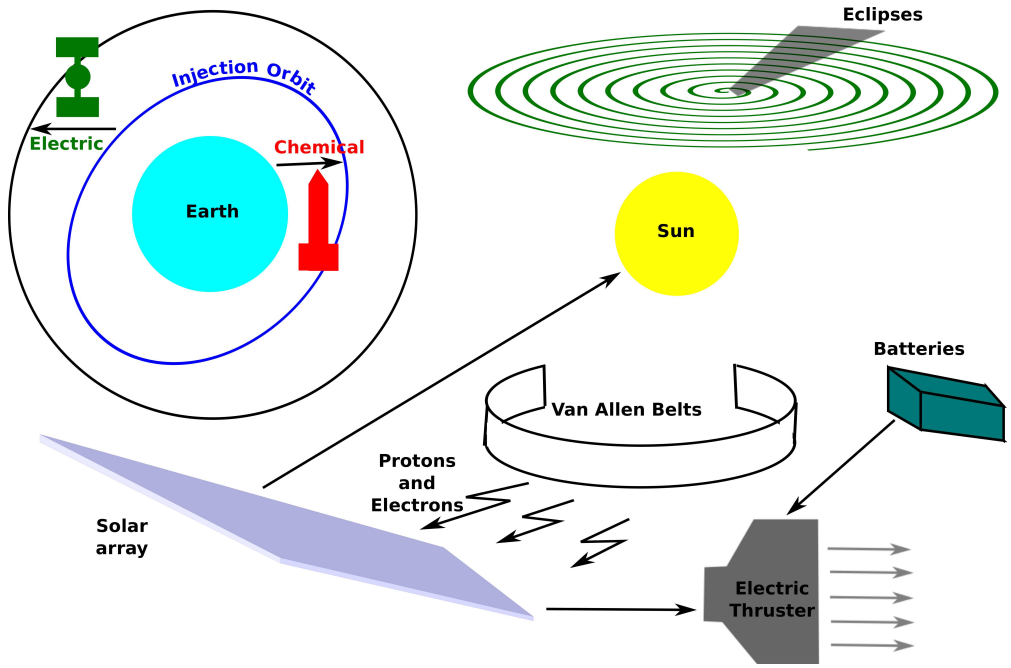

Figure 1. Important aspects of an electric orbit-raising mission design problem.

during the transfer), type of electric thrustes (such as Hall or ion thrusters), energy storage (provides limited or full thrusting capability during eclipses). Combining the variety of technology alternatives, a mission designer needs to investigate hundreds of scenarios, each of which require the solution of a challenging non-linear, multi-phase optimal control problem associated with the complex orbit-raising maneuver.

Over the years, two prominent methods for solving the optimal control problem associated with low-thrust transfers have evolved. One approach considers the application of calculus of variations in order to identify the analytic necessary conditions of optimality,[1] and constructing the corresponding two-point boundary value problem that is solved numerically.[2,3,4,5,6] This approach is referred to as the indirect optimization approach. Alternatively, one can discretize the state and control variables with respect to time and apply quadrature rules across the discretized segments in order to set up a parameter optimization problem that can be solved efficiently using efficient non-linear programming solvers such as SNOPT, IPOPT or KNITRO.[7,8,9,10] Owing to the explicit avoidance of the necessary conditions of optimality, these methods are referred to as direct optimization techniques. While numerical schemes based on direct methods are acknowledged to demonstrate better convergence characteristics compared to their indirect counterparts, both direct and indirect methods need some form of user-provided initial guesses to kick-start the optimization problem, thereby hindering automated computation of low-thrust orbit-raising trajectories. In order to address this deficiency, a number of studies investigated alternate non-optimal approaches, such as shape-based methods and guidance-based scheme,[11,12,13,14,15,16,17,18,19,20,21,22,23,24] which can be used as good initial guesses for a direct or indirect optimization scheme. A number of different dynamic models of the maneuvering spacecraft has been used to study the orbit-raising problem, and Ref. 25 provides a comparison of a variety of dynamic models, specifically for their influence on the convergence of numerical optimization

schemes for computing the low-thrust trajectory. Through a comparison with a variety of state variable choices, it was demonstrated in this study that a set of newly introduced regularized elements (introduced in Ref. **?**) is efficient for the low-thrust orbit-raising problem. The key to the novel dynamic model is the use of dynamical parameters (as opposed to geometrical quantities) as the state variables of the spacecraft, and the use of a non-inertial reference frame that can be obtained using a 2-1-3 rotation sequence of Euler angles, instead of the traditional 3-1-3 rotation sequence used in orbital mechanics (Figure 2). An advantage

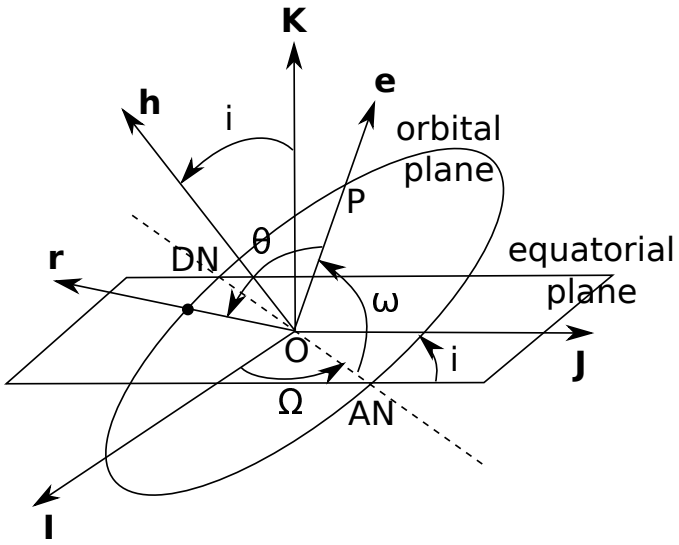

Figure 2. *Traditional orbital elements.*

of the dynamic model over traditional orbital elements is that the singularity of traditional orbital elements no longer exists for either equatorial or circular orbits. In fact, the singularity is transferred to special cases of polar orbits when the right ascension of the ascending node of the orbit is 0 or 2π deg. Another key advantage of the new orbital element set is that they are regularized variables, five of which are constant for Keplerian motion, and change slowly under the action of perturbations. Hence, they are suitable for use in trajectory optimization schemes that compute long-time-scale transfers.

Reference 26 also considered an optimization scheme that breaks up the multi-revolution problem into a sequence of optimization sub-problems in order to generate the electric orbit-raising trajectory; this methodology allows the computation of the electric orbit-raising trajectory in the order of tens of seconds on a standard personal computer, without the need for any user-inputed initial guess. The formulation has the benefit of being used as an automated tool to analyze numerous electric orbit-raising mission scenarios without the need for intervention by the user. In addition, the formulation is non-singular in the equatorial plane, thereby facilitating the computation of the trajectories ending up in GEO. However, the solutions are sub-optimal, and it was demonstrated in Ref. 26 that the optimality gap is larger for starting elliptic orbits such as geosynchronous transfer orbit (GTO), sub-GTO and super-GTO, compared to starting circular orbits in low-Earth orbits (LEO). With the goal of reducing the optimality gap, we take a closer look at the low-thrust sequential optimization sub-problems, whose objective function has three components (two in the case of planar transfers) combined using a convex combination of weights. Considering that the local objective

function (for an optimization sub-problem) does not imply global optimality of an objective (transfer time for the entire maneuver), this paper investigates the effect of weights on the transfer time of the orbit-raising maneuvers. A variety of orbit-raising mission scenarios are studied and numerical simulations are used to identify values of weights (and range of those values) that should be used by a mission designer in order to yield the least transfer time.

ELECTRIC ORBIT-RAISING PROBLEM FORMULATION

We denote the spacecraft position vector with respect to the celestial body by $\boldsymbol{r}$ and the velocity vector by $\boldsymbol{v}$. The equations of translational motion of the spacecraft relative to the Earth can be written as:

$$\dot{\boldsymbol{r}} = \boldsymbol{v}, \quad \dot{\boldsymbol{v}} = -\frac{\mu}{r^3}\boldsymbol{r} + \boldsymbol{p} \tag{1}$$

where r is the radial distance (magnitude of $\boldsymbol{r}$), μ is Earth's gravitational parameter due to gravity at the surface of the Earth, $\boldsymbol{p}$ constitutes the accelaration due to all non-keplerian forces (thrust and orbital perturbations). In the context of the current paper, we do not consider any perturbation, hence, $\boldsymbol{p}$ only represents the thrust force. When we have $\boldsymbol{p} = \mathbf{0}$ (no thrust), the resulting spacecraft trajectory is a conic section constrained in a plane. Furthermore, the following dynamical parameters are constant: the specific angular momentum vector $\mathbf{h} = \boldsymbol{r} \times \boldsymbol{v}$ that is normal to orbit plane, the eccentricity vector $\boldsymbol{e} = \boldsymbol{v} \times \boldsymbol{h}/\mu - \boldsymbol{r}/r$ that lies on the orbit plane and is directed towards the closest approach, and specific energy $\epsilon = \boldsymbol{v} \cdot \boldsymbol{v} - \mu/r$. As explained in the previous section, the dynamic model used in this paper focusses on the use of dynamic parameters to represent the state of the spacecraft. To this end, we consider that the following constitute the states of the spacecraft: the magnitude of the specific angular momentum vector h, the components h_X and h_Y of the specific angular momentum vector in the X-Y plane of the Earth-centered inertial reference frame $\mathcal{I}$, the components e_x and e_y of the eccentricity vector of the $x-y$ plane of the non-inertial reference frame obtained by 2-1 rotation, and the true anomaly-like angle ϕ determining the location of the spacecraft in orbit from an inertially fixed plane (X-Z). The sign of h_Z is assumed to always be positive, that is typical of all prograde (typical) spacecraft orbits. At any instant of time, the position and velocity vectors are uniquely defined if the proposed states are known. The first five elements of the state vector are constant under Keplerian motion, and varies slowly under the action of low thrust, hence, the elements are regularized. The last element (angle ϕ) is the only fast variable, and for the purpose of optimization, is considered to be the decision variable (instead of time). Hence, we club the first five elements together as $\boldsymbol{x}$ and then represent the dynamic model in the following form:

$$\begin{bmatrix} \dot{\mathbf{x}} \\ \dot{\phi} \end{bmatrix} = \boldsymbol{f}(\boldsymbol{x}, \phi) + \mathbf{G}(\boldsymbol{x}, \phi)\,\boldsymbol{p}, \tag{2}$$

$$\boldsymbol{f} = \left[0, 0, 0, 0, 0, \frac{\mu^2 B^2}{h^3}\right]^T, \quad A_j = e_x \sin\phi_j - e_y \cos\phi_j, \quad B_j = 1 + e_x \cos\phi_j + e_y \sin\phi_j, \tag{3}$$

$$\mathbb{G} = \begin{bmatrix} 0 & \frac{h^2}{\mu m B} & 0 \\ 0 & \frac{h h_X}{\mu m B} & \frac{h^2\sqrt{h^2-h_X^2-h_Y^2}}{\mu m B\sqrt{h^2-h_Y^2}}\sin\phi + \frac{h h_X h_Y}{\mu m B\sqrt{h^2-h_Y^2}}\cos\phi \\ 0 & \frac{h h_Y}{\mu m B} & -\frac{h\sqrt{h^2-h_Y^2}}{\mu m B}\cos\phi \\ \frac{h\sin\phi}{\mu m} & \frac{2h\cos\phi}{\mu m} + \frac{hA\sin\phi}{\mu m B} & \frac{h e_y h_Y \sin\phi}{\mu m B\sqrt{h^2-h_Y^2}} \\ -\frac{h\cos\phi}{\mu m} & \frac{2h\sin\phi}{\mu m} - \frac{hA\cos\phi}{\mu m B} & -\frac{h e_x h_Y \sin\phi}{\mu m B\sqrt{h^2-h_Y^2}} \\ 0 & 0 & -\frac{h h_Y \sin\phi}{\mu m B\sqrt{h^2-h_Y^2}} \end{bmatrix}. \tag{4}$$

Note that the resulting low-thrust transfer trajectory is a slowly developing spiral comprised of numerous revolutions (of the order of hundreds or thousands). Our approach is to set up a sequence of optimization sub-problems, where each sub-problem is defined by one revolution, during which the angle ϕ changes by an amount 2π. The goal of each sub-problem is to move the spacecraft as close to GEO as possible at the end of the revolution. Note that, the GEO (or any orbit for that matter) can be defined by its specific angular momentum of magnitude h_{GEO} and directed along $\hat{\boldsymbol{K}}$, and its eccentricity of 0. Let the state vector at the end of the revolution achieved by the optimized trajectory (by solving the optimization sub-problem) be denoted by the sub-script 'end' for the associated variables. The goal is to ensure the following: (1) the magnitude of the angular momentum is as close to that of GEO as possible, (2) the eccentricity is as close to that of GEO as possible, (3) the unit vector in the direction of the angular momentum is as aligned to $\hat{\boldsymbol{K}}$ as possible. Note that, the magnitude of the projection of the angular momentum onto the (inertial) equatorial plane (X-Y) is given by $h_{X,end}^2 + h_{Y,end}^2$; when the angular momentum is exactly aligned to $\hat{\boldsymbol{K}}$, the magnitude of the projection equals zero. The objective is written as a convex combination of the three component mentioned above:

$$J = \min\left[w_h(h_{GEO} - h_{end})^2 + w_e(e_{x,end}^2 + e_{y,end}^2) + w_{hxy}(h_{X,end}^2 + h_{Y,end}^2)\right], \tag{5}$$

where w_h, w_e and w_{hxy} are the relative weights for the individual objectives with $w_h + w_e + w_{hxy} = 1$. Clearly, the third component has no use when the transfer starts from an equatorial orbit leading to a planar low-thrust transfer. Hence, for the special case of planar transfers, we will set $w_{hxy} = 0$.

Without loss in generality, we assume that the transfer is initiated for the first time when the spacecraft passes through the inertial X-Z plane in its starting orbit. Evidently, this means that our initial ϕ is zero. Each revolution can therefore be considered to begin at an integral multiple of 2π. Given these considerations, we can say that the angle $\phi \in [0, 2\pi]$ during each revolution. We discretize the trajectory over each segment into $n+1$ nodes and denote by ϕ_j the angles demarcating the discretized nodes, where $j = 0, \ldots, n$. We therefore have:

$$\phi_j = \frac{2\pi}{n} j.$$

During each revolution, the states h, h_x, h_y e_x and e_y are assumed to be approximately constant, meaning that the trajectory during each revolution will approximately represent the shape of a conic section (typically an ellipse for an electric orbit-raising problem). Figure (3) depicts the discretization of the trajectory over one revolution. Next, we need to identify which of these nodes will be in eclipse. The shadow geometry

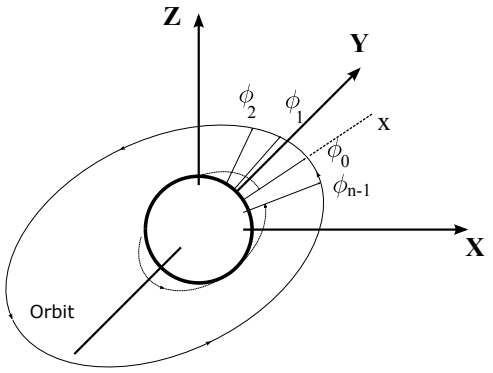

Figure 3. Segmentation of the trajectory over a revolution.

is assumed to be of cylindrical geometry with the radius equalling that of the Earth and the length infinite. The shadow direction points away from the center of the Earth, opposite to the direction of the Sun. For the purpose of the current paper, we ignore the rotation of the Earth about the Sun, that is, we assume that the shadow orientation does not change over time. The shape of the eclipse is described in Figure 4. We can

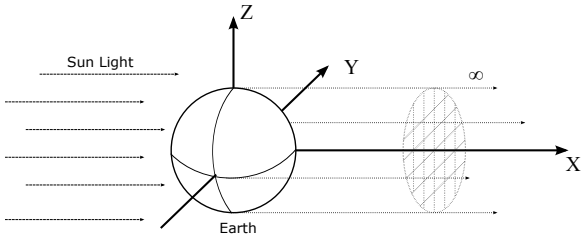

Figure 4. Segmentation of an elliptical orbit.

then determine the nodes that will be in eclipses during a revolution by finding the set of all points on the trajectory satisfying the shadow conditions $\mathcal{S}$ (please see Ref. 26 for the details on these computations):

$$\mathcal{E} = \{\, j \in \{0, 1, 2, \ldots, (n-1)\} |\, \boldsymbol{x}_j \in \mathcal{S}\} \tag{6}$$

Obviously, the segments that are in the sun-lit portion of the trajectory are given by:

$$\mathcal{T} = \{\, j \in \{0, 1, 2, \ldots, (n-1)\} |\, \boldsymbol{r}_j, \boldsymbol{r}_{j+1} \notin \mathcal{S}\}\,, \tag{7}$$

and the spacecraft is sure to thrust over these segments (because our global objective is to minimize the transfer time during the maneuvers).

Note that the dynamic model (Eq. (2)) has the system description with respect to the time variable, however, for the purpose of solving each optimization sub-problem, we need to understand how the slow state variables change with respect to the fast variable ϕ. The dynamics of the spacecraft is therefore written with respect to the angle ϕ (sixth element) as follows:

$$\frac{d}{d\phi}\left[\begin{array}{ccccc} h & h_X & h_Y & e_x & e_y \end{array}\right]^T = \frac{dt}{d\phi}\left[\begin{array}{ccccc} \dot{h} & \dot{h}_X & \dot{h}_Y & \dot{e}_x & \dot{e}_y \end{array}\right]^T, \tag{8}$$

where the derivative $dt/d\phi$ is the inverse of the relationship described by the sixth equation in Eq. (2), that is,

$$\frac{dt}{d\phi} = \frac{1}{\dot{\phi}} = \frac{h^3 m\mu B\sqrt{h^2 - h_Y^2}}{m\mu^3 B^3\sqrt{h^2 - h_Y^2} - h^4 h_Y \sin\phi F_h}, \tag{9}$$

where F_h is the out-of-plane force component. The Eq. (9) is non-linear, however, we assume that the component of the thrust F_h to be small, we perform a linearization of the above equation and obtain the following:[26]

$$\frac{dt}{d\phi} \approx \left.\frac{dt}{d\phi}\right|_{F_h=0} + \left.\frac{\partial}{\partial F_h}\left(\frac{dt}{d\phi}\right)\right|_{F_h=0} F_h = \frac{h^3}{\mu^2 B^2} + \frac{h^7 h_Y \sin\phi}{m\mu^5\sqrt{h^2 - h_Y^2}B^5} F_h. \tag{10}$$

Now, for each node given by $j \in \{0, 1, \ldots, n\}$, the rates of change of the state variables can be calculated using Eq. (8) and Eq. (10), as shown below:

$$\begin{bmatrix} \frac{dh}{d\phi} \\ \frac{dh_X}{d\phi} \\ \frac{dh_Y}{d\phi} \\ \frac{de_x}{d\phi} \\ \frac{de_y}{d\phi} \end{bmatrix} \approx \frac{h^3}{\mu^2 B^2}\mathbf{C}\begin{bmatrix} F_r \\ F_n \\ F_h \end{bmatrix} + \frac{h^7 h_Y \sin\phi}{m\mu^5\sqrt{h^2 - h_Y^2}B^5}\mathbf{C}\begin{bmatrix} F_r F_h \\ F_n F_h \\ F_h^2 \end{bmatrix}, \tag{11}$$

where the matrix C is derived from Eq. (2) and given by

$$\mathbf{C} = \begin{bmatrix} 0 & \frac{h^2}{\mu m B} & 0 \\ 0 & \frac{hh_X}{\mu m B} & \frac{h^2\sqrt{h^2-h_X^2-h_Y^2}}{\mu m B\sqrt{h^2-h_Y^2}}\sin\phi + \frac{hh_X h_Y}{\mu m B\sqrt{h^2-h_Y^2}}\cos\phi \\ 0 & \frac{hh_Y}{\mu m B} & -\frac{h\sqrt{h^2-h_Y^2}}{\mu m B}\cos\phi \\ \frac{h\sin\phi}{\mu m} & \frac{2h\cos\phi}{\mu m} + \frac{hA\sin\phi}{\mu m B} & \frac{he_y h_Y \sin\phi}{\mu m B\sqrt{h^2-h_Y^2}} \\ -\frac{h\cos\phi}{\mu m} & \frac{2h\sin\phi}{\mu m} - \frac{hA\cos\phi}{\mu m B} & -\frac{he_x h_Y \sin\phi}{\mu m B\sqrt{h^2-h_Y^2}} \end{bmatrix}. \tag{12}$$

The trapezoidal rule of integration is then used to determine the action of the thrust force over each segment under the assumption of constant thrust magnitude F_k over each segment $[\phi_k, \phi_{k+1}]$, resulting in the following:

$$\begin{bmatrix} \tilde{h}_k \\ \tilde{h}_{X,k} \\ \tilde{h}_{Y,k} \\ \tilde{e}_{x,k} \\ \tilde{e}_{y,k} \end{bmatrix} \approx \frac{\phi_{k+1} - \phi_k}{2}\left(\begin{bmatrix} \frac{dh}{d\phi} \\ \frac{dh_X}{d\phi} \\ \frac{dh_Y}{d\phi} \\ \frac{de_x}{d\phi} \\ \frac{de_y}{d\phi} \end{bmatrix}_k + \begin{bmatrix} \frac{dh}{d\phi} \\ \frac{dh_X}{d\phi} \\ \frac{dh_Y}{d\phi} \\ \frac{de_x}{d\phi} \\ \frac{de_y}{d\phi} \end{bmatrix}_{k+1}\right), \tag{13}$$

which, on the application of Eq. (41), becomes

$$\begin{bmatrix} \tilde{h}_k \\ \tilde{h}_{X,k} \\ \tilde{h}_{Y,k} \\ \tilde{e}_{x,k} \\ \tilde{e}_{y,k} \end{bmatrix} \approx \frac{\pi}{n} \left(\frac{h^3}{\mu^2 B_k^2} \mathbf{C}_k \begin{bmatrix} F_r \\ F_n \\ F_h \end{bmatrix}_k + \frac{h^7 h_Y \sin\phi_k}{m\mu^5 \sqrt{h^2 - h_Y^2} B_k^5} \mathbf{C}_k \begin{bmatrix} F_r F_h \\ F_n F_h \\ F_h^2 \end{bmatrix}_k \right.$$
$$\left. + \frac{h^3}{\mu^2 B_{k+1}^2} \mathbf{C}_{k+1} \begin{bmatrix} F_r \\ F_n \\ F_h \end{bmatrix}_k + \frac{h^7 h_Y \sin\phi_{k+1}}{m\mu^5 \sqrt{h^2 - h_Y^2} B_{k+1}^5} \mathbf{C}_{k+1} \begin{bmatrix} F_r F_h \\ F_n F_h \\ F_h^2 \end{bmatrix}_k \right). \tag{14}$$

Note here that $\tilde{h}_k$, $\tilde{h}_{X,k}$, $\tilde{h}_{Y,k}$, $\tilde{e}_{x,k}$ and $\tilde{e}_{y,k}$ are the changes of the state variables along the segment k owing to the applied thrust. The value of the state variables at the end of the revolution can be simply obtained by summing up the changes over all segments as given below:

$$\begin{bmatrix} h & h_X & h_Y & e_x & e_y \end{bmatrix}_{end}^T = \begin{bmatrix} h & h_X & h_Y & e_x & e_y \end{bmatrix}^T + \sum_{k=0}^{n-1} \begin{bmatrix} \tilde{h}_k \\ \tilde{h}_{X,k} \\ \tilde{h}_{Y,k} \\ \tilde{e}_{x,k} \\ \tilde{e}_{y,k} \end{bmatrix}. \tag{15}$$

The magnitude of the thrust force at each node can be written as one of three cases:

$$F_k = \begin{cases} F, \text{ if } k \in \mathcal{T}, \\ 0, \text{ if } k \notin \mathcal{T} \text{ and the spacecraft does not thrust during eclipses .} \end{cases} \tag{16}$$

The direction of the thrust defined by angles at each segment α_k and β_k serve as the decision variables for the optimization sub-problem. Hence, the control input vector at the node k can be written as:

$$\begin{bmatrix} F_r \\ F_n \\ F_h \end{bmatrix}_k = \begin{bmatrix} F \sin\alpha_k \cos\beta_k \\ F \cos\alpha_k \cos\beta_k \\ F \sin\beta_k \end{bmatrix}. \tag{17}$$

The mass at the end of the revolution can be computed as:

$$m_{end} = m - \frac{\pi F}{n I_{sp} g_0} \sum_{k \in \mathbb{T}} \left(\frac{h^3}{\mu^2 B_k^2} + \frac{h^3}{\mu^2 B_{k+1}^2} + \frac{h^7 h_Y \sin\phi_k F \sin\beta_k}{m\mu^5 \sqrt{h^2 - h_Y^2} B_k^5} + \frac{h^7 h_Y \sin\phi_{k+1} F \sin\beta_{k+1}}{m\mu^5 \sqrt{h^2 - h_Y^2} B_{k+1}^5} \right) \tag{18}$$

Note that the formulated optimization problem is an unconstrained one, and is more robust and faster to solve than a similar-dimensional constrained optimization problem. Once this optimization sub-problem is solved, the state variables at the end of the revolution are used to provide the initial states for the next

revolution, and the sequence is continued until the spacecraft reaches the GEO. In order to determine when the spacecraft reaches GEO, we set the stopping conditions as follows:

$$0 \leq \sqrt{e_{x,end}^2 + e_{y,end}^2} \leq e_{tol}, \tag{19}$$

$$a_{GEO} - a_{tol} \leq \frac{h_{end}^2}{\mu(1 - e_{x,end}^2 - e_{y,end}^2)} \leq a_{GEO} + a_{tol}, \tag{20}$$

$$0 \leq \sqrt{\frac{h_{x,end}^2 + h_{y,end}^2}{h}} \leq \sin\left(i_{tol}\right), \tag{21}$$

where e_{tol}, a_{tol} and i_{tol} are the acceptable eccentricity, semi-major axis and inclination angle tolerances of the GEO, respectively. Note that the use of both upper and lower bounds in the stopping criteria may lead to a case of chattering when the objective function over successive iterations may fluctuate around the GEO. This can be avoided in one of two ways: either use bounds on one direction (either a lower or upper bound) or stop the algorithm if a chattering event is detected. We use chattering detection in our methodology. The overall algorithm is depicted in the flowchart given in Fig. 5.

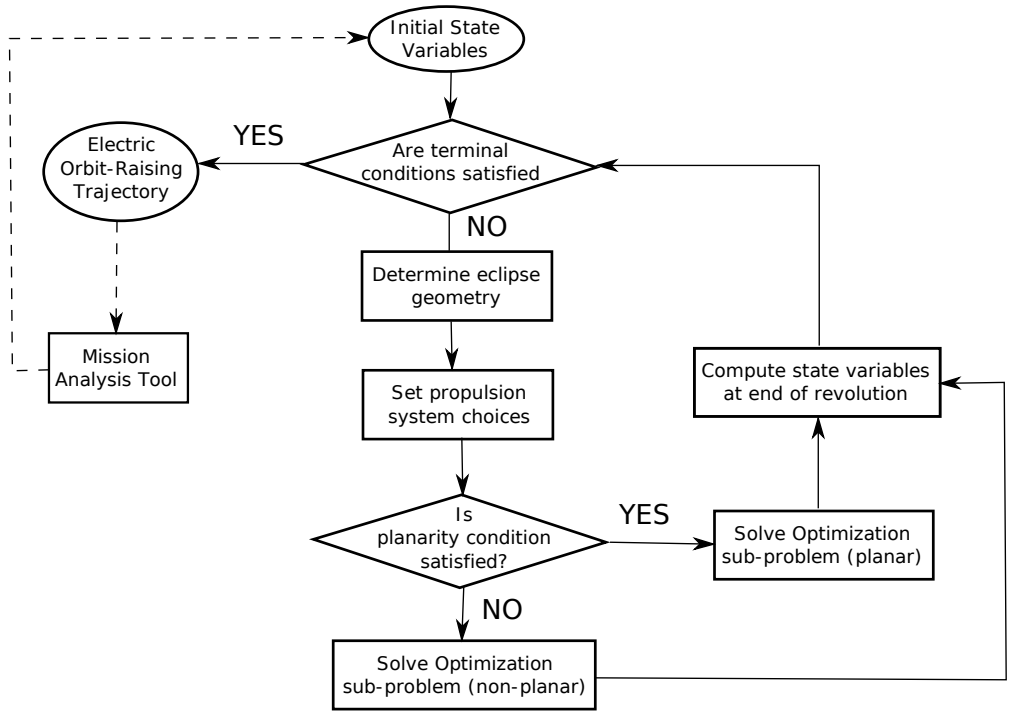

Figure 5. Algorithm flowchart and interaction with a mission analysis tool.

PLANAR ORBIT-RAISING SCENARIOS

In this section, we consider orbit-raising maneuvers starting from equatorial orbits (LEO, sub-GTO, GTO and super-GTO) and perform a parametric study in order to investigate the effect of weights on the orbit-

raising transfer time. The considered maneuvers are planar low-thrust transfers; hence, the selection of w_h completely describes the objective function because $w_{hxy} = 0$ and $w_e = 1 - w_h$. Accordingly, we consider the solution of 100 orbit-raising problems for each starting conditions (initial orbits) by varying w_h linearly between 0.1 and 0.99.

Circular LEO to GEO planar transfer We consider that a 5000 kg spacecraft initiates the transfer from a circular orbit of altitude of 2000 km. A number of orbit-raising scenarios are then considered corresponding to the different values of w_h. Figure 6(a) shows the variation of the transfer time with the considered values of w_h. It is observed that the trajectory computed with w_h = 0.6933 gives the least transfer time of 215.2 sidereal days, a final mass of 3984.6 kg and a total of 1117 revolutions. When compared to the case when the weights are equal (w_h = w_e = 0.50), the transfer time is found to be 216.72 sidereal days, a final mass of 3975.55 kg and a total of 1135 revolutions. By following a slightly heavier weighting of w_h, there is a marginal reduction in transfer time by 0.74%.

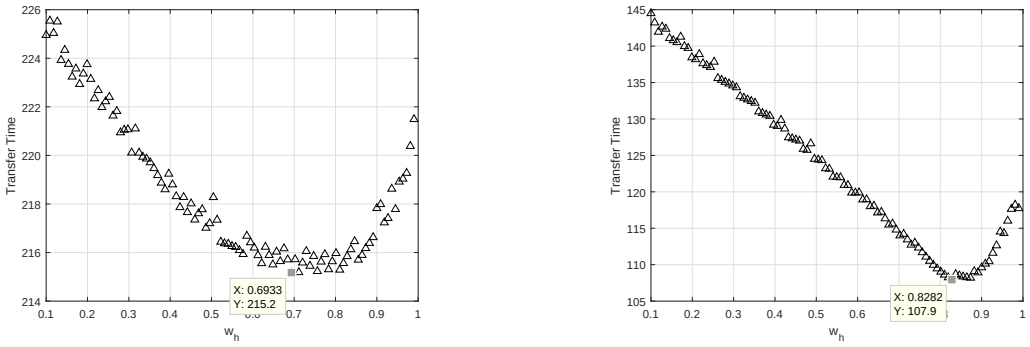

(a) LEO to GEO (b) GTO to GEO

Figure 6. Variation of transfer time with w_h for planar transfers.

GTO to GEO Planar Transfer The initial orbit of the spacecraft is considered to be a GTO with a perigee altitude of 250 km. Naturally, the apogee altitude is 35786 km. Initial value of the mass of the spacecraft is considered to be 5000 kg. For this scenario, a number of orbit-raising transfer problems are generated for linearly space choices of w_h between 0.1 and 0.99. Figure 6(b) shows the variation of the transfer time with the considered values of w_h. Among all transfers considered, the trajectory with w_h = 0.8788 was found to yield the minimum transfer time of 108.37 sidereal days, a final mass of 4409.05 kg and a total of 158 revolutions. Compared to the scenario when weights are equal (that is, $w_h = w_e$ = 0.50), the transfer time is 124.96 sidereal days, final mass is 4328.72 kg, and the transfer is completed over 228 revolutions. By significantly increasing the relative weighting for the angular momentum difference (high w_h), there is a substantial reduction in the transfer time of 13.27% .

Next, we investigate the effect of the perigee altitude on the best choice of w_h corresponding to the least transfer time. To this end, we consider different planar GTO with the following perigee altitudes: 250 km, 1000 km, 2000 km, 5000 km, 10000 km. The results are summarized in Table 1. The results demonstrate that increasing the perigee of the starting orbit means a corresponding decrease in the weight w_h in the objective function in order to yield the least transfer time.

Table 1. Summary of results for variation of initial perigee of equatorial GTO.

Initial Perigee (km)	Transfer Time (sidereal days)	w_h	w_e
250	108.37	0.8788	0.1212
1000	103.37	0.8417	0.1583
2000	98	0.8231	0.1769
5000	83.3	0.8602	0.1398
10000	63.44	0.8417	0.1583

Sub-GTO to GEO Planar Transfer The initial orbit is a sub-GTO with a perigee altitude of 250 km and an apogee altitude of 30000 km. Initial value of the mass of the spacecraft is taken to be 5000 kg. For this scenario, multiple orbit-raising problems are solved for linearly-spaced vector w_h varying between 0.1 and 0.99. Figure 7(a) depicts the variation of the corresponding transfer time with respect to chosen values of w_h for these transfers. Of those computed trajectories, the one with w_h = 0.8788 yields the minimum transfer time of 113.4 sidereal days, a final mass of 4384.96 kg after completing a total of 191 revolutions. Compared to the least transfer time solution, an equal weighting of the individual objectives ($w_h = w_e$ = 0.50) result in a transfer time of 133.46 sidereal days, a final mass of 4288.98 kg, and a total of 282 revolutions. By a heavier weighting of w_h, there is a considerable reduction in transfer time by 15.03% .

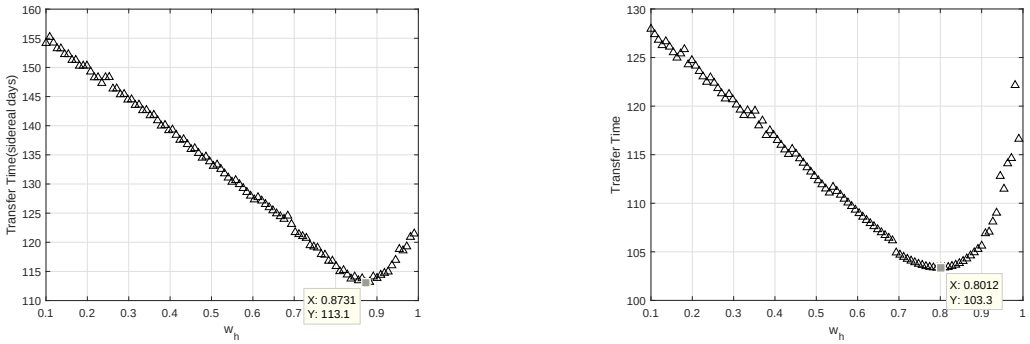

(a) sub-GTO to GEO (b) super-GTO to GEO

Figure 7. Variation of transfer time with w_h for planar transfers.

Next, we investigate the effect of the apogee altitude of the initial sub-GTO on the best choice of w_h corresponding to the least transfer time. To this end, we consider different planar sub-GTO with the following apogee altitudes: 5000 km, 10000 km, 20000 km, 30000 km. The results are summarized in Table 3. The results demonstrate that increasing the apogee of the starting orbit means a corresponding decrease in the weight w_h in the objective function in order to yield the least transfer time.

Super-GTO to GEO Planar Transfer The initial orbit for this scenario is a super-GTO with a perigee altitude of 250 km and an apogee altitude of 45000 km. Initial value of the mass of the spacecraft is taken

Table 2. Summary of results for variation of initial apogee of equatorial sub-GTO.

Initial Apogee (km)	Transfer Time (sidereal days)	w_h	w_e
30000	113.4	0.8788	0.1212
20000	127.91	0.8602	0.1398
10000	158.60	0.9344	0.0656
5000	195.95	0.9158	0.0842

to be 5000 kg, as in previous examples. For this scenario, a number of orbit-raising transfer trajectories are computed for linearly spaced vector w_h varying between 0.1 and 0.99. Figure 7(b) depicts the variation of the corresponding transfer time with respect to chosen values of w_h for these transfers. Out of these computed low-thrust orbit-raising trajectories, the one corresponding to w_h = 0.7860 gives the least transfer time of 102.67 sidereal days, a final mass of 4438.89 kg and a total of 135 revolutions. Comparing to the solution for equal weighting of the two components of the objective function ($w_h = w_e$ = 0.50) with the transfer time of 113.07 sidereal days, a final mass of 4386.57 kg and a total of 168 revolutions), we find that there is a reduction in transfer time for super-GTO scenario by 9.26% by following a non-equal weighting of the objective function components.

Next, we investigate the effect of the apogee altitude of the initial super-GTO on the best choice of w_h corresponding to the least transfer time. Hence, we consider different planar starting super-GTOs with the following apogee altitudes: 45000 km, 50000 km, 55000 km, 60000 km. The results are summarized in Table 3. The results demonstrate that increasing the apogee of the starting orbit means a corresponding

Table 3. Summary of results for variation of initial apogee of equatorial super-GTO.

Initial Apogee (km)	Transfer Time (sidereal days)	w_h	w_e
45000	102.67	0.7860	0.2140
50000	101.10	0.7860	0.2140
55000	100.3	0.6933	0.3067
60000	99.46	0.5079	0.4921

decrease in the weight w_h in the objective function in order to yield the least transfer time. The changes in w_h required are more prominent, compared to the scenarios when the transfer starts from a sub-GTO (varying apogee) or a GTO (varying perigee).

NONPLANAR TRANSFERS

In this section, we consider orbit-raising maneuvers starting from non-equatorial orbits (LEO, sub-GTO, GTO and super-GTO) and perform a parametric study in order to investigate the effect of weights on the orbit-raising transfer time, similar to the previous section on planar transfers. The considered maneuvers

are non-planar low-thrust transfers; hence, the selection of at least two of the three weights is required for completely describing the objective function. Accordingly, we consider $24^2 = 576$ orbit-raising problems generated by linearly spaced vectors w_h and w_{hxy} between 0.1 and 0.99. Note that the selection of w_h and w_{hxy} automatically determines $w_e = 1 - w_h - w_{hxy}$.

Circular LEO to GEO Nonplanar Transfer In this case, we consider the spacecraft to be initially in a circular LEO of 2000 km altitude and an inclination of 28.5 deg. Similar to the planar transfers, we take the initial mass of the spacecraft to be 5000 kg. Based on the chosen selection of weights, 576 orbit-raising trajectories are computed for equally spaced values of w_h and w_{hxy} varying between 0.1 and 0.99. Figure 8(a) depicts the variation of the corresponding transfer time with respect to chosen values of w_h and w_{hxy} for these transfers. Of these transfer trajectories, the one with w_h = 0.4870 and w_{hxy} = 0.4483 gives the least transfer time of 238.02 sidereal days, a final mass of 3741.10 kg and a total of 1114 revolutions. Compared to the case of equal weighting of the three components of the objective function for the non-planar transfer (w_h = 1/3, w_{hxy} = 1/3) that corresponds to a transfer time of 241.29 sidereal days and a final mass of 3733.28 kg (a total of 1146 revolutions), we see that there is a marginal reduction in transfer time for by 1.35%.

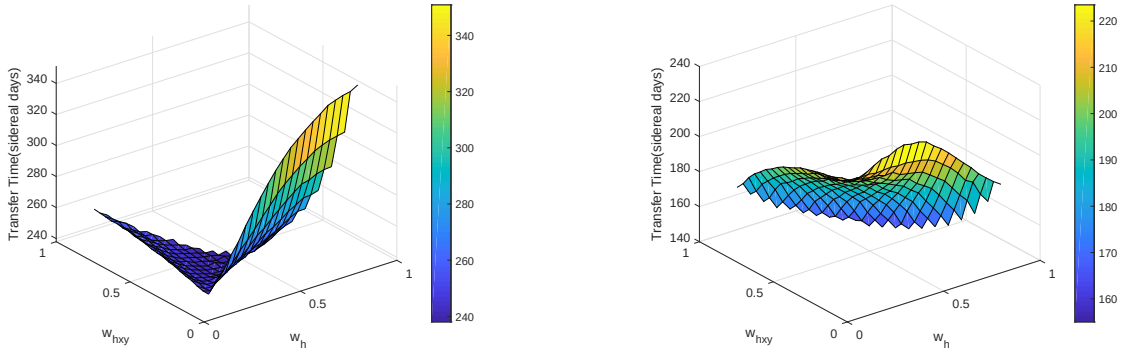

(a) LEO to GEO

(b) GTO to GEO

Figure 8. Variation of transfer time with w_h and w_{hxy} for non-planar transfers.

GTO to GEO Nonplanar Transfer In this case, we consider spacecraft initially to be in a perigee altitude of 250 km and an apogee altitude of 35786 km with an inclination of 28.5 deg. Similar to planar transfers, we consider the initial mass of the spacecraft to be 5000 kg. For the considered nonplanar transfer scenario, 576 orbit-raising instances are solved, considering linearly spaced values of w_h and w_{hxy} varying between 0.1 and 0.99. Figure 8(b) depicts the variation of the corresponding transfer time with respect to chosen values of w_h and w_{hxy} for these transfers. Out of those trajectories, the one with w_h = 0.4400 and w_{hxy} = 0.5257 gives the least transfer time of 155.91 sidereal days, a final mass of 4134.28 kg and a total of 225 revolutions. Compared to the case of equal weighting (w_h = 0.3333, w_{hxy} = 0.3333) that yields a transfer time of 190.46 sidereal days, a final mass of 3933 kg and a total of 335 revolutions, the unequal weighting of the objective function components yield a a 18.14 % reduction in transfer time.

Sub-GTO to GEO Nonplanar Transfer In this case, we consider spacecraft initially to be in a perigee altitude of 250 km and an apogee altitude of 30000 km with an inclination of 28.5 deg. Similar to the planar transfers, we take the initial mass of the spacecraft to be 5000 kg. We solve 576 orbit-raising problems based on equally spaced values of w_h and w_{hxy} varying between 0.1 and 0.99. Figure 9(a) depicts the variation of the corresponding transfer time with respect to chosen values of w_h and w_{hxy} for these transfers. Out of those trajectories, trajectory with w_h = 0.4400 and w_{hxy} = 0.5250 gives the least transfer time of 161.60 sidereal days, a final mass of 4105.74 kg and a total of 265 revolutions. When compared to the solution yielded by an equal weighting of the components of the objective function (w_h = 0.3333, w_{hxy} = 0.3333, transfer time of 197.24 sidereal days, final mass of 3897.84 kg and total of 394 revolutions), we find that unequal weighting scheme can lead to a reduction in transfer time by 18.07%.

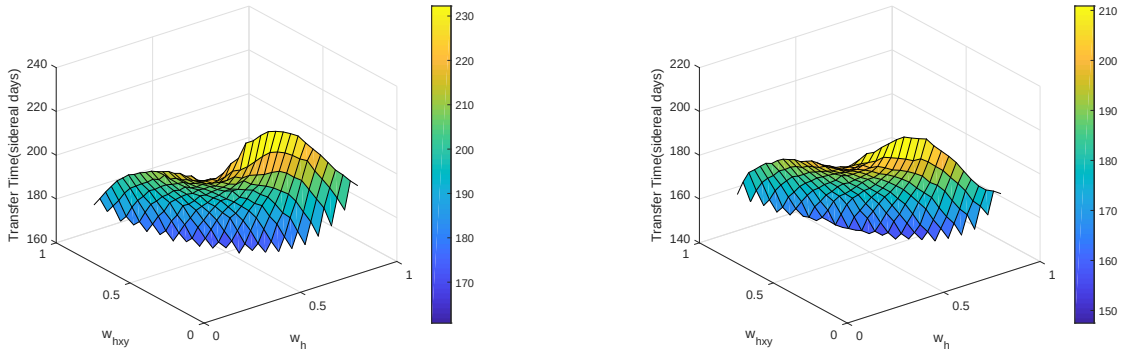

(a) sub-GTO to GEO

(b) super-GTO to GEO

Figure 9. Variation of transfer time with w_h and w_{hxy} for non-planar transfers.

Super-GTO to GEO Nonplanar Transfer In this case, we consider spacecraft initially to be in a perigee altitude of 250 km and an apogee altitude of 45000 km with an inclination of 28.5 deg, with the initial mass of the spacecraft to be 5000 kg. We solve a number of orbit-raising problems generated for linearly spaced values of w_h and w_{hxy} varying between 0.1 and 0.99, and Fig. **??** depicts the variation of the corresponding transfer time with respect to chosen values of w_h and w_{hxy} for these transfers. Out of those trajectories, trajectory with w_h = 0.40 and w_{hxy} = 0.55 gives the minimum transfer time of 150.09 sidereal days, a final mass of 4166 kg and a total of 193 revolutions as compared to w_h = 0.3333 and w_{hxy} = 0.3333 with the transfer time of 181.86 sidereal days, a final mass of 3978.87 kg and a total of 269 revolutions. By adjusting w_h and w_{hxy}, there is a reduction in transfer time for by 17.47%.

A summary of the numerical results is provided in Table 4.

CONCLUSIONS

In this paper, we studied the low-thrust orbit-raising problem and consider a recently developed optimization scheme that poses the multi-phase non-linear optimal control problem as a sequence of optimal control sub-problems. This formulation utilizes a novel dynamic model that ensures a rapid and robust computations of electric orbit-raising trajectories without the need for user-provided initial guesses. This advantage comes

Table 4. Summary of Results

Starting orbit	Transfer time (sidereal days)	w_h	w_e	w_{hxy}	Final mass (kg)
Planar transfers					
LEO (2000 km $\times$ 2000 km altitude)	215.2	0.6933	0.3067	0	3984.6
GTO (250 km $\times$ 35786 km)	107.9	0.8282	0.1718	0	4413.38
Sub-GTO (250 km $\times$ 30000 km)	113.1	0.8731	0.1269	0	4387.24
Super-GTO (250 km $\times$ 45000 km)	103.34	0.8012	0.1988	0	4434.96
Nonplanar Transfer (i = 28.5 deg)					
Circular LEO (250 km $\times$ 35786 km)	238.02	0.4870	0.0647	0.4483	3741.10
GTO (250 $\times$ 35786 km)	155.91	0.4400	0.0343	0.5257	4134.28
Sub-GTO (250 km $\times$ 30000 km)	161.60	0.4400	0.035	0.5250	3897.84
Super-GTO (250 km $\times$ 45000 km)	150.09	0.40	0.05	0.55	4166

at the cost of sub-optimality of the computed solutions, because we do not directly minimize transfer time. Instead, the objective function that is minimized in each optimal control sub-problem is a convex combination of three components (two in the case of planar transfers) that reflect the deviation of the maneuvering spacecraft from the geosynchronous equatorial orbit (GEO). This paper explores the impact of weights on the objective function components on the transfer times associated with the computed orbit-raising trajectories. A parametric study is conducted by considering linearly spaced choices on the weights in the objective function, and a variety of planar and non-planar mission scenarios are concerned. It is observed that unequal weighting of the objectives only improves the transfer time marginally if the initial orbit is circular. However, in the case of elliptic starting orbits, the transfer times are significantly improved in the case of GTO, sub-GTO and super-GTO transfers. Furthermore, it is observed that the choice of the optimal weighting scheme (corresponding to least transfer time) is also influenced by the orbit characteristics, such as perigee of the GTO, apogee of the sub-GTO and super-GTO. In this cases, our study helps in identifying the range of values over which the weight can be chosen by a mission designer.

REFERENCES

[1] D. Lawden, *Optimal Trajectories for Space Navigation*. Butterworths, London, 1963.

[2] M. W. Marasch and C. D. Hall, "Application of Energy Storage to Solar Electric Propulsion Orbital Transfer," *Journal of Spacecraft and Rockets*, Vol. 37, Sep-Oct 2000, pp. 645–652.

[3] C. H. Ferrier and R. Epenoy, "Optimal Control for Engines with Electro-Ionic Propulsion under Constraint of Eclipse," *Acta Astronautica*, Vol. 48, No. 4, 2001, pp. 181–192.

[4] C. A. Kluever, "Geostationary Orbit Transfers Using Solar Electric Propulsion with Specific Impulse Modulation," *Journal of Spacecraft and Rockets*, Vol. 41, No. 3, 2004, pp. 461–466.

[5] B. N. Kiforenko, "Optimal low-thrust orbital transfers in a central gravity field," *International Applied Mechanics*, Vol. 41, No. 11, 2005, pp. 1211–1238, 10.1007/s10778-006-0028-9.

[6] R. Russell, "Primer Vector Theory Applied to Global Low-Thrust Trade Space Studies," *Journal of Guidance, Control and Dynamics*, Vol. 30, No. 2, 2007, p. 2.

[7] C. A. Kluever and S. R. Oleson, "Direct approach for computing near-optimal low-thrust earth-orbit transfers," *Journal of Spacecraft and Rockets*, Vol. 35, No. 4, 1998, pp. 509–515.

[8] R. Falck and J. Dankanich, "Optimization of Low-Thrust Spiral Trajectories by Collocation," *AIAA/AAS Astrodynamics Specialist Conference, Guidance, Navigation, and Control and Co-located Conferences*, Minneapolis, MN, August 2012.

[9] A. Dutta, P. Libraro, N. J. Kasdin, and E. Choueiri, "A Direct Optimization Based Tool to Determine Orbit-Raising Trajectories to GEO for All-Electric Telecommunication Satellites," *AAS Astrodynamics Specialist Conference*, Minneapolis, MN, Aug 2012.

[10] K. F. Graham and A. V. Rao, "Minimum-Time Trajectory Optimization of Low-Thrust Earth-Orbit Transfers with Eclipsing," *Journal of Spacecraft and Rockets*, Vol. 53, March–April 2016, pp. 289–303.

[11] T. N. Edelbaum, "Propulsion requirements for controllable satellites," *ARS Journal*, Vol. 31, No. 8, 1961, pp. 1079–1089.

[12] G. A. Flandro, "Asymptotic Solution for Solar Electric Low-Thrust Orbit Raising with Eclipse Penalty," *AIAA Mechanics and Control of Flight Conference*, Anaheim, CA, Aug 5-9 1974.

[13] W. Wiesel and S. Alfano, "Optimal Many-Revolution Orbit Transfer," *Journal of Guidance, Control and Dynamics*, Vol. 8, January–February 1985, pp. 155–157.

[14] J. A. Kechichian, "Low-Thrust Eccentricity-Constrained Orbit Raising," *Journal of Spacecraft and Rockets*, Vol. 35, May-June 1998, pp. 327–335.

[15] J. A. Kechichian, "Orbit Raising with Low-Thrust Tangential Acceleration in Presence of Earth Shadow," *Journal of Spacecraft and Rockets*, Vol. 35, July-Aug 1998, pp. 516–525.

[16] J. A. Kechichian, "Low-Thrust Inclination Control in Presence of Earth Shadow," *Journal of Spacecraft and Rockets*, Vol. 35, July-Aug 1998, pp. 526–532.

[17] C. Kluever, "Simple Guidance Scheme for Low-Thrust Orbit Transfers," *Journal of Guidance, Control, and Dynamics*, Vol. 21, No. 6, 1998, pp. 1015–1017.

[18] A. E. Petropoulos, "Simple Control Laws for Low-thrust Orbit Transfers," *AIAA/AAS Astrodynamics Specialist Conference*, Big Sky, MT, August 2003.

[19] G. Colasurdo and L. Casalino, "Optimal Low-Thrust Maneuvers in Presence of Earth Shadow," *AIAA/AAS Astrodynamics Specialist Conference and Exhibit*, Providence, RI, August 2004.

[20] B. Wall and B. Conway, "Shape-Based Approach to Low-Thrust Rendezvous Trajectory Design," *Journal of Guidance, Control, and Dynamics*, Vol. 32, January–February 2009, pp. 95–101.

[21] C. Kluever, "Using Edelbaums Method to Compute Low-Thrust Transfers with Earth-Shadow Eclipses," *Journal of Guidance, Control and Dynamics*, Vol. 34, January–February 2011, pp. 300–303.

[22] E. Taheri and O. Abdelkhalik, "Shape-Based Approximation of Constrained Low-Thrust Space Trajectories Using Fourier Series," *Journal of Spacecraft and Rockets*, Vol. 49, May–June 2012, pp. 535–545.

[23] R. D. Falck, W. K. Sjauw, and D. A. Smith, "Comparison of Low-Thrust Control Laws for Applications in Planetocentric Space," *50th AIAA/ASME/SAE/ASEE Joint Propulsion Conference*, Cleveland, OH, July 2014.

[24] J. T. Betts, "Optimal low–thrust orbit transfers with eclipsing," *Optimal Control Applications and Methods*, Vol. 36, No. 2, 2015, pp. 218–240.

[25] J. L. Junkins and E. Taheri, "Exploration of Alternative State Vector Choices for Low-Thrust Trajectory Optimization," *Journal of Guidance, Control, and Dynamics*, Vol. 42, January 2019, pp. 47–64.

[26] S. Sreesawet and A. Dutta, "Fast and Robust Computation of Low-Thrust Orbit-Raising Trajectories," *AIAA Journal of Guidance, Control and Dynamics*, Vol. 41, Sep 2018, pp. 1888–1905.